Drawing of poly(vinyl alcohol) gel films

Po-Da Hong and Keizo Miyasaka
Department of Organic and Polymeric Materials, Tokyo Institute of Technology, Meguro-ku, Tokyo 152, Japan
(Received 14 June 1990; revised 19 July 1990; accepted 4 August 1990)

The drawability and physical properties of dried poly(vinyl alcohol) (PVA) gel films prepared from *N*-methylpyrrolidone (NMP) and ethyleneglycol (EG) solutions were compared. X-ray diffraction and differential scanning calorimetry showed that PVA/EG gels had higher values of crystallinity than PVA/NMP gels. The drawability of dried PVA/NMP gels was higher than that of PVA/EG gels at all drawing temperatures. Although the maximum draw ratio of dried PVA/NMP gel films increased with molecular weight, the extent of the increase is much less than in the case of polyethylene gel films, partly because the highest molecular weight available in this study was lower than in the case of ultra-high-molecular weight polyethylene. The highest draw ratio achieved was about 28× for a dried PVA/NMP ($DP = 14400$, 2 wt%) gel film and its tensile strength and modulus were 1 GPa and 30 GPa, respectively. The α_c relaxation temperature (T_{α_c}) of PVA shifted to high temperature with increasing draw ratio, approaching the melting point, while the second-order crystal transition point remained at 120°C. This implies that the α_c relaxation is related to molecular motion in the crystal–amorphous boundary.

(Keywords: poly(vinyl alcohol); gel film; drawability; physical properties; mechanical relaxation)

INTRODUCTION

Since the gel spinning of ultra-high-molecular-weight polyethylene (UHMWPE) has been developed[1], many researchers have attempted to develop high-performance fibrous materials from other flexible semicrystalline polymers such as poly(vinyl alcohol) (PVA)[2–9].

Owing to the *trans* conformation, the PVA crystal has a modulus in the chain direction as high as 250 GPa[10]. Atactic PVA is crystallizable and at the same time makes thermoreversible gels in many solutions such as water[11], ethyleneglycol (EG)[2], dimethylsulphoxide (DMSO)[9], *N*-methylpyrrolidone (NMP)[12] and mixtures of these solvents[13]. High drawing is necessary to get high-modulus and high-strength fibrous materials. The drawability of dried PVA gels must be affected by the structure and properties, and depends greatly on the molecular weight and the species of the solvents.

In this work we first studied the structure and properties of PVA gels from EG and NMP solutions, and the drawability and the properties of drawn specimens were studied for PVA/NMP gel films, which were found to have higher drawability than PVA/EG gels. Furthermore, the second-order crystal transition reflecting the crystalline chain mobility, the α_c mechanical relaxation and the relation between them and drawability of PVA gel films were discussed.

EXPERIMENTAL

Sample preparation

A 99% hydrolysed commercial medium-molecular-weight PVA ($DP = 2000$, Wako Chem. Co., Japan) and high-molecular-weight PVAs ($DP = 4800$, 7900, 12900 and 14400, kindly provided by Kuraray Co.) were used in this work. These PVAs were dissolved in EG and NMP at 120–130°C for 2 h. The homogeneous solutions were poured into aluminium trays to make gels at room temperature. The gels were washed with methanol, and then dried in a vacuum oven at 50°C for one day. These dried gel films, whose thickness was about 200 μm, were drawn in silicone oil at a given temperature using a manual stretching apparatus.

Characterization methods

Wide-angle X-ray diffraction (WAXD) photographs were taken by a flat camera with Ni-filtered CuKα radiation from a Rigaku XG working at 35 kV and 20 mA. The WAXD and small-angle X-ray scattering (SAXS) intensities were measured using a scintillation counter with a pulse height analyser in a Rigaku Rota Flex RU200 working at 50 kV and 180 mA. The crystal orientation function f_c of drawn samples was estimated by the azimuthal scanning of the (020) reflection (the chain axis is parallel to the *b* axis)[14]. The thickness of the crystal was estimated from the breadth of the (020) reflection using the Scherrer equation[15,16]. The breadth was corrected for the measuring condition, using silicone powder. The long spacing was evaluated from the SAXS intensity peak maximum.

The thermal expansion of the PVA crystal lattice was measured using WAXD equipped with a high-temperature sample holder over a temperature range of 20 to 220°C at a scan speed 0.25° min^{-1}.

D.s.c. measurements were carried out using a Shimadzu DT-40 at a heating rate of 10°C min^{-1}. Crystallinity was estimated from the area of the d.s.c. melting peak, using 37.5 cal g^{-1} (156.2 J g^{-1})[17,18] as the heat of fusion of PVA crystal.

The tensile modulus and strength were estimated from stress–strain curves using a Tensilon (UTM-II-20, Toyo

0032-3861/91/173140-07

Baldwin Co. Ltd) at a strain rate of 6.7×10^{-3} s^{-1} in an atmosphere controlled at 20°C and r.h. 50%.

The dynamic mechanical properties were measured at a frequency of 10 Hz using a Rheovibron (Toyo Seiki Co., Japan) over a temperature range from 0 to 260°C, at a heating rate of 3°C min^{-1}, in a N_2 atmosphere.

RESULTS AND DISCUSSION

Figures 1a and *1b* show WAXD photographs of PVA/NMP and PVA/EG wet gels. Although a large part of the intensity is the contribution of solvents, comparison of these WAXD photographs indicates that PVA/EG gel has a higher crystallinity than PVA/NMP gel. The properties of these two gels are compared in *Table 1*. Gelation of both solutions occurred in a couple of seconds at room temperature. PVA/NMP gels were transparent, while PVA/EG gels were milky white. PVA/NMP gels had much higher elasticity compared with PVA/EG gels. Syneresis was observed within a few hours in PVA/EG gels, while no noticeable syneresis occurred for PVA/NMP gels within several days. The melting point of PVA/EG gels, which tended to shift to a higher temperature with increased syneresis, was higher than that of PVA/NMP gels. The degrees of swelling in water at 20°C of dried PVA/EG gel films were smaller than those of PVA/NMP films. This indicates that a thicker network structure is formed in dried PVA/EG gels than in PVA/NMP gels.

These differences in the structure and properties of PVA gels due to the species of solvents are related to their different affinities to PVA, i.e. the solubility of PVA in NMP is larger than that in EG[12,19]. It is known that only solvents such as diols and triols having structures similar to PVA result in PVA single crystals and that PVA crystallizes from a dilute EG solution[20], but not from an NMP solution[12]. X-ray diffraction and turbidity of PVA/EG gels indicated that a number of crystals formed during the gelation, making aggregates large enough to scatter visible light. This aggregation may be the same as that proposed by Berghmans[21]. The transparency and high elasticity of PVA/NMP gels are considered to be due to the low crystallinity and less crystal aggregation.

Table 1 General features of PVA/NMP and PVA/EG gels ($DP \approx 2000$, conc. 8 wt%)

	PVA/NMP	PVA/EG
Gelation rate	Fast	Fast
Appearance	Transparent	Milky white
Elasticity	High	Low
Syneresis	Very slow	Fast
Melting point	100°C	125°C
Swelling degree in water of dried gel	300%	250%

Figure 2 shows the effect of drawing temperature on the maximum draw ratio λ_{max} defined as the highest draw ratio achieved under a given drawing condition for dried PVA/NMP and PVA/EG gel films prepared from 8 wt% solutions. The value of λ_{max} of dried PVA/NMP gel films is larger than that of dried PVA/EG gels at all drawing temperatures. There are three regions in the λ_{max} *versus* drawing temperature relation: $\lesssim$80°C, 80–160°C, $\gtrsim$160°C. The increase in λ_{max} becomes remarkable over 80°C, related possibly to the glass transition, and less remarkable above 160°C. The value of λ_{max} depends on the plasticity and breaking strength of a specimen under a given draw condition. The main reason for the less remarkable increases in λ_{max} above 160°C is due to the decrease in the strength.

Figure 3 shows the crystal orientation function f_c of samples drawn in silicone oil at 200°C. The crystal orientation is almost perfect at draw ratios over 10×, and there is no significant difference between PVA/NMP and PVA/EG gel films, except that a 5× drawn PVA/NMP gel has a higher f_c than a similar PVA/EG gel film. The smaller f_c of PVA/EG gels at low draw ratios is considered to be due to the larger degrees of crystallinity and crystal aggregation.

Figures 4a and *4b* show respectively the draw ratio dependences of tensile modulus and strength for the same dried gel films as in *Figure 3*. Both values increase with increasing draw ratio. At a given draw ratio, the tensile modulus of PVA/NMP samples is higher than that of PVA/EG. This may be attributed to the homogeneous structure of PVA/NMP gel films before drawing as mentioned above. On the other hand, there is no

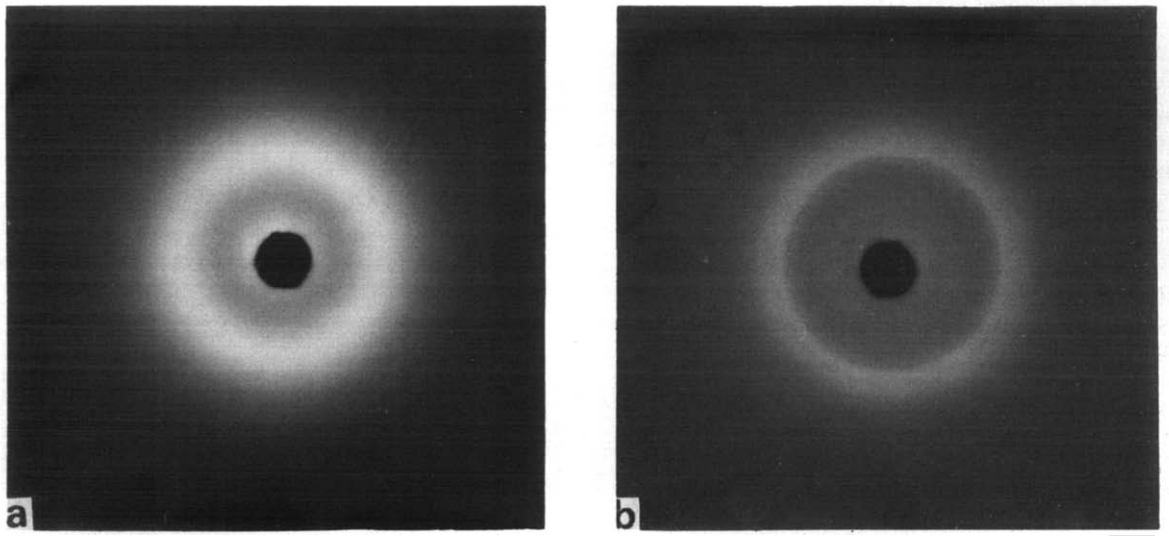

Figure 1 WAXD photographs of wet gels: (a) PVA/NMP gel; (b) PVA/EG gel

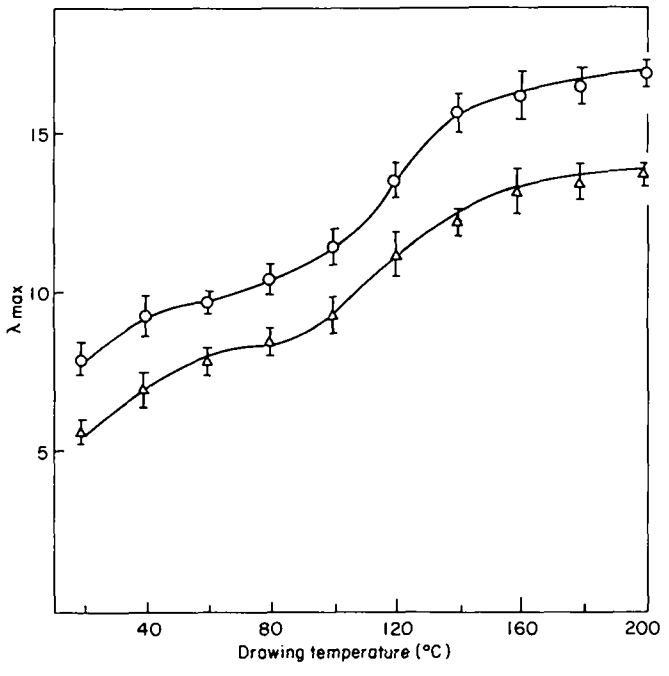

Figure 2 Maximum draw ratio as a function of drawing temperature for $DP = 2000$, 8 wt% dried gel film: (○) PVA/NMP, (△) PVA/EG

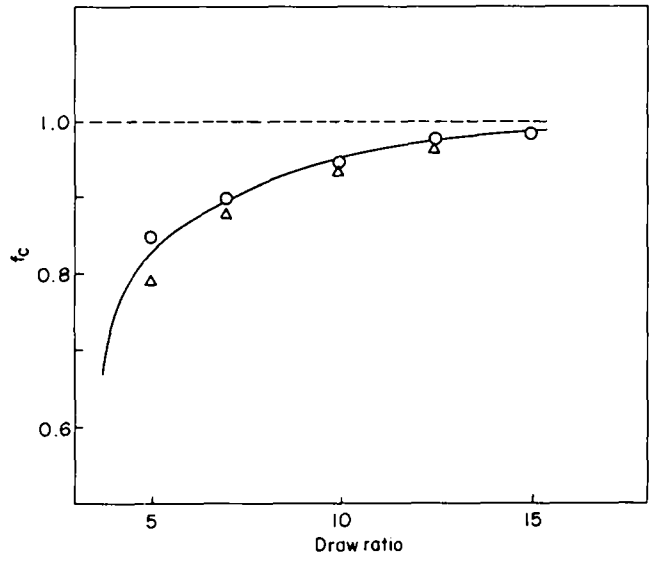

Figure 3 Crystal orientation function f_c as a function of draw ratio. All descriptions correspond to the same samples as in *Figure 2*

difference in the tensile strength. The combination of *Figures 3* and *4* indicates that at a given f_c the PVA/NMP sample has a higher modulus than the PVA/EG sample, emphasizing the importance of structure in the original dried gel films. From these results, hereafter our attention is concentrated only on PVA/NMP gel films to study the drawability and physical properties of drawn films.

Figure 5 shows λ_{max} of dried 2 wt% PVA/NMP gel films drawn at 200°C as a function of MW. The value of λ_{max} increases slightly with increasing MW, and the highest value of λ_{max} achieved in this study was 28 × for $MW = 63 \times 10^4$ ($DP = 14\,400$) and 18 × for $MW = 9 \times 10^4$ ($DP = 2000$). It should be noted that the largest MW (63×10^4) of PVA available in this study was much less than that of UHMWPE used in the same kind of studies for PE.

Figures 6a and *6b* show respectively the draw ratio dependences of the tensile modulus and strength of $DP = 14\,400$ and 2000 samples. Both tensile modulus and strength increase with draw ratio. At a given draw ratio, the higher MW samples have higher tensile modulus and strength. Cracks along the drawing direction were formed in lower MW samples above a draw ratio of 15 ×. The tensile strength and modulus of a 25 × drawn film of PVA/NMP gel ($DP = 14\,400$, 2 wt%) were 1 GPa and 30 GPa.

In *Figure 7* the tensile strength is plotted against the tensile modulus for drawn dried gel films of two different MW samples. The plot satisfies a relationship given by equation (1) as is known for gel-spun UHMWPE reported by Smith *et al.*[22]:

$$\sigma = mE^n \quad (1)$$

where σ and E are the tensile strength and modulus, and

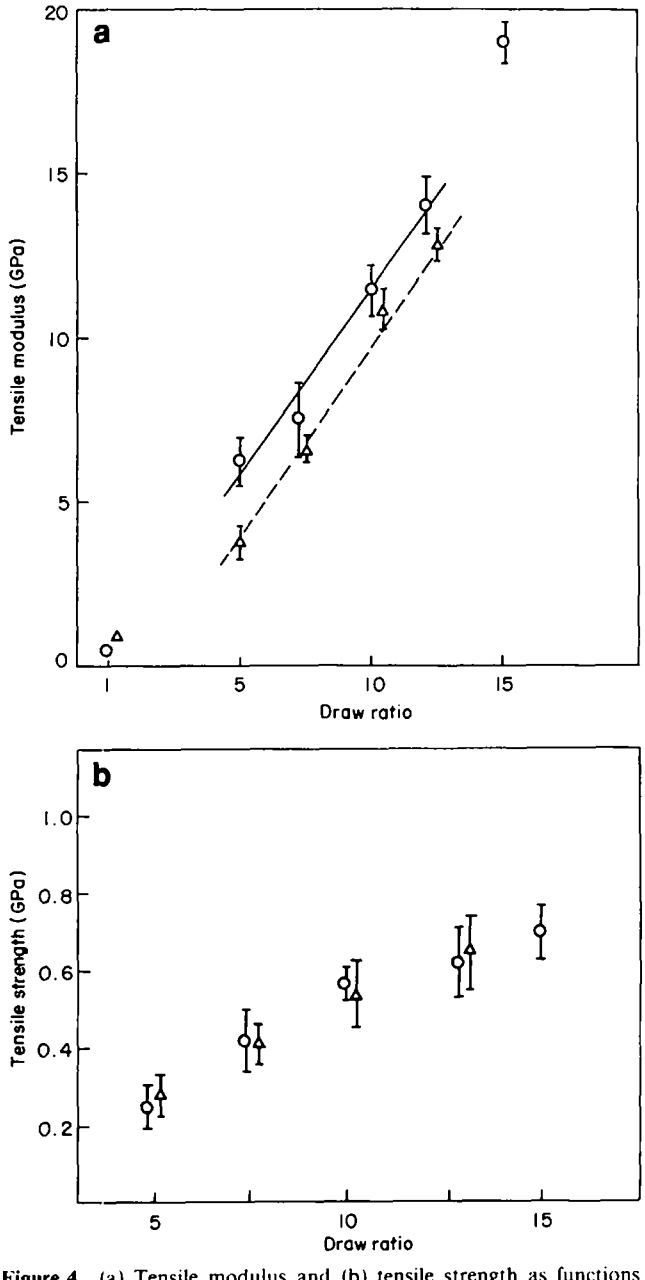

Figure 4 (a) Tensile modulus and (b) tensile strength as functions of draw ratio. All descriptions correspond to the same samples as in *Figure 2*

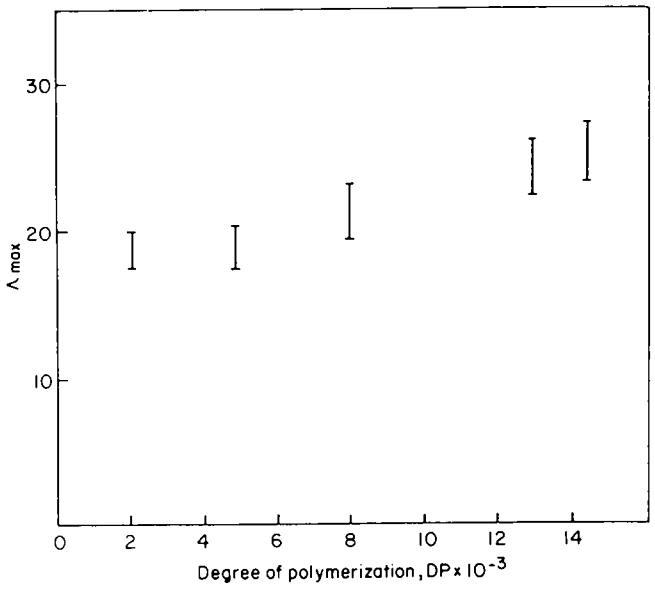

Figure 5 The maximum draw ratio λ_{max} as a function of degree of polymerization DP for 2 wt% PVA/NMP samples drawn at 200°C

m and n are constants. The values of m and n are 0.110 and 0.67 for the $MW = 63.4 \times 10^4$ ($DP = 14.4 \times 10^3$) samples, and 0.079 and 0.65 for the $MW = 8.8 \times 10^4$ ($DP = 2 \times 10^3$) samples: m increases with MW, while n remains constant at about 0.65. It is interesting to note that these results are similar to those of UHMWPE reported by Smith *et al.*[22], where m changes from 0.082 to 0.153 with change in MW from 80×10^4 ($DP = 28.5 \times 10^3$) to 400×10^4 ($DP = 142.8 \times 10^3$), while n remains constant at about 0.77.

Figure 8 shows the change of the SAXS profile with drawing. The peak corresponding to the long period appears clearly in the 5× sample, but weakens and becomes broader in highly drawn samples. Since the SAXS peak intensity is proportional to the square of the density difference of crystalline and amorphous phases, the result of *Figure 8* indicates that the density difference tends to decrease with drawing, which is due to the increase in the density of the amorphous phase. However, the peak does not disappear even at the highest draw ratio, indicating that samples still had a crystalline amorphous two-phase in-series structure. *Figure 9* shows

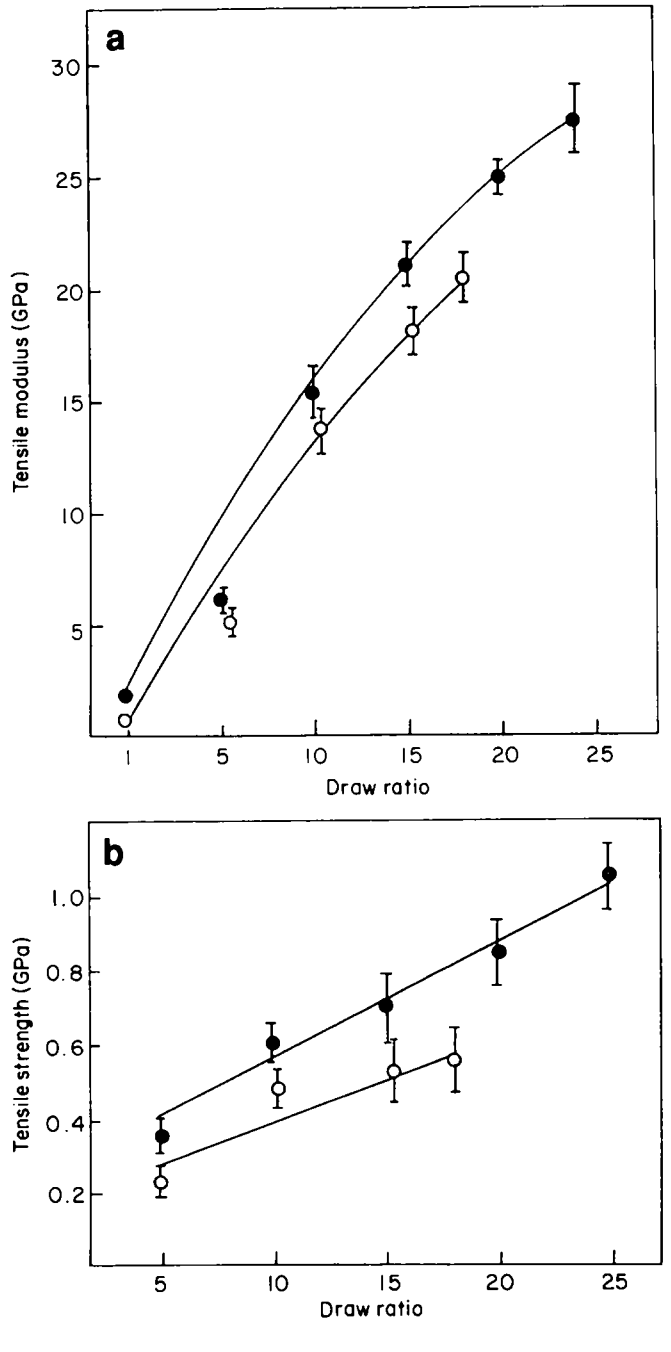

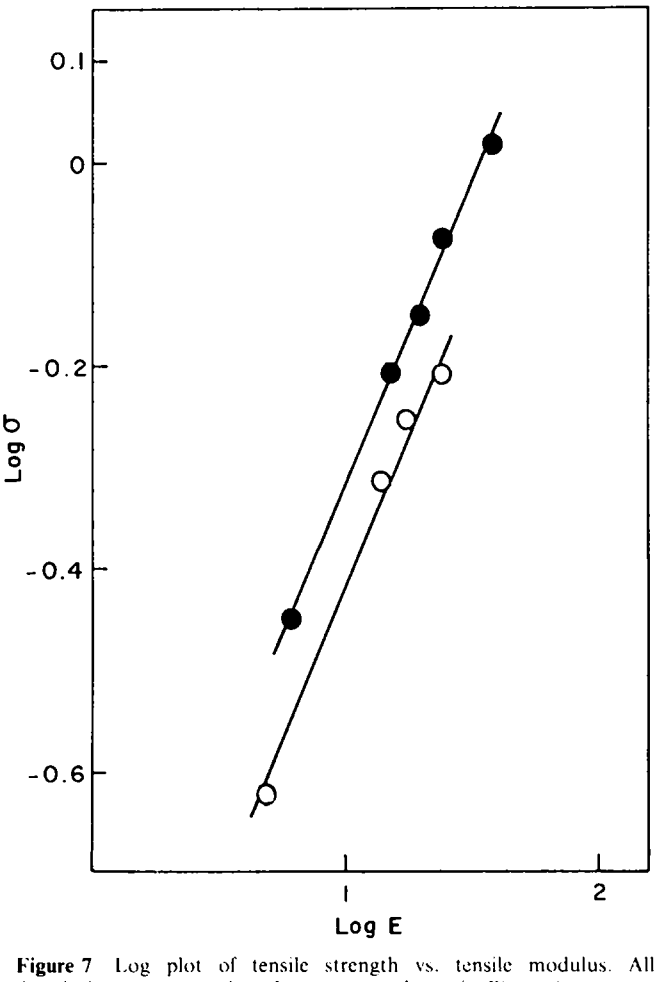

Figure 7 Log plot of tensile strength vs. tensile modulus. All descriptions correspond to the same samples as in *Figure 6*

Figure 6 (a) Tensile modulus and (b) tensile strength as a function of draw ratio for 2 wt% PVA/NMP samples: (●) $DP = 14400$, (○) $DP = 2000$

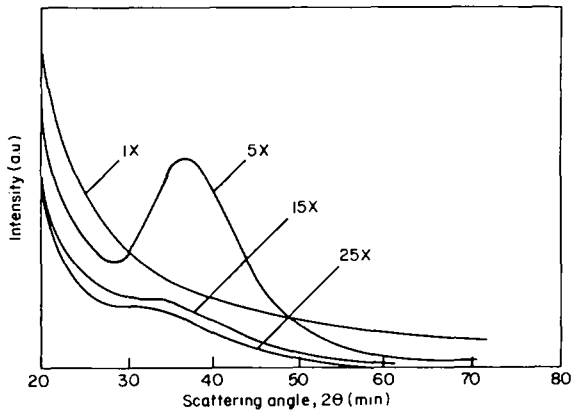

Figure 8 The changes of SAXS intensity curve as a function of draw ratio for $DP = 14\,400$, 2 wt% PVA/NMP samples

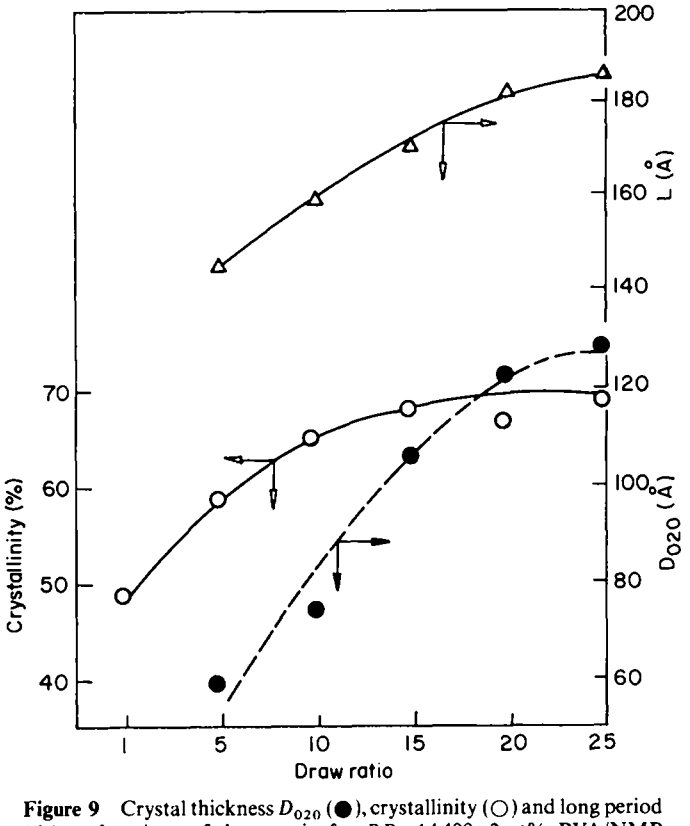

Figure 9 Crystal thickness D_{020} (●), crystallinity (○) and long period (△) as functions of draw ratio for $DP = 14\,400$, 2 wt% PVA/NMP samples

crystallinity, crystal thickness D_{020} and long period L as functions of draw ratio. All of them increase with increasing draw ratio.

Figure 10 shows the dynamic storage modulus E' as a function of temperature. The E' curves of the specimens of different draw ratios have a similar temperature dependence, although the rate of decrease at high temperatures is somewhat less at higher draw ratios. The range of the plateau appearing at low temperatures increases with increasing draw ratio, indicating the shift of T_g to higher temperature.

Figure 11 shows the change of tan δ with temperature at different draw ratios. Two peaks in the tan δ *versus* temperature curves appear at all draw ratios except 25×. The low-temperature peak due to T_g shifts slightly to higher temperatures, which may be due to an increase in the packing density of amorphous chains and also to an increase in the crystallinity. Furthermore, the α_c relaxation peak shifts to high temperatures and disappears at 25×. The α_c relaxation temperature (T_{α_c}) was 170°C and 230°C for the undrawn and 20× drawn samples, respectively. This change has already been reported by Garrett *et al.*[23] for PVA films drawn by the zone-drawing technique.

Figure 12 shows the melting point T_m determined by d.s.c. and T_{α_c} as functions of draw ratio. T_{α_c} shifts to higher temperatures with increasing draw ratio, approaching T_m at high draw ratios.

Garrett *et al.* considered that the disappearance of the α_c relaxation at high draw ratios is one reason for difficulty in high drawing of PVA. Furthermore, they attributed the shift of T_{α_c} to a decrease in the mobility of crystalline chains due to an increase of crystal thickness with drawing, because the α_c relaxation is related to molecular motion in the crystalline region. It is well known that the thermal expansion coefficient of PVA crystal lattice changes discontinuously at about 120°C[24], and that the crystal has a second-order transition point at this temperature. This temperature corresponds to the crystal relaxation temperature of 130°C reported by Takayanagi *et al.*[25]. If the α_c relaxation is uniquely related to molecular motion of the crystalline region, the shift of T_{α_c} caused by drawing seen in *Figure 11* must be followed by a shift of the second-order crystal transition point. Under this expectation, the thermal expansion of crystals was measured for the same drawn samples as in *Figure 11*.

Figures 13a and *13b* show the temperature variations in the (1 0 0) and (0 1 0) spacings of PVA crystal for the

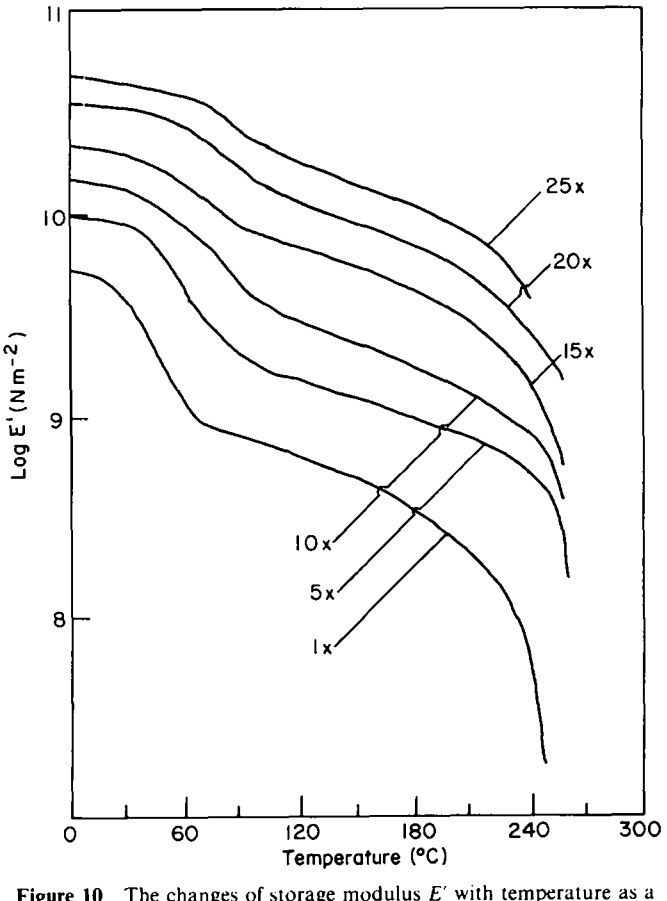

Figure 10 The changes of storage modulus E' with temperature as a function of draw ratio for $DP = 14\,400$, 2 wt% PVA/NMP samples

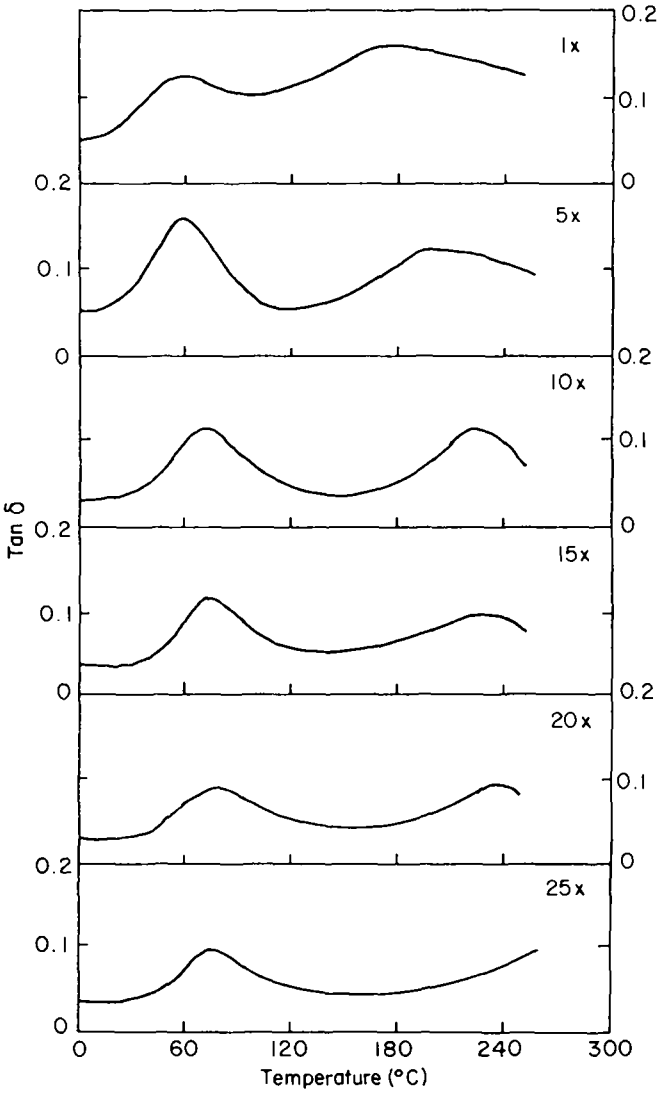

Figure 11 The changes of mechanical tan δ with temperature as a function of draw ratio for $DP = 14400$, 2 wt% PVA/NMP samples

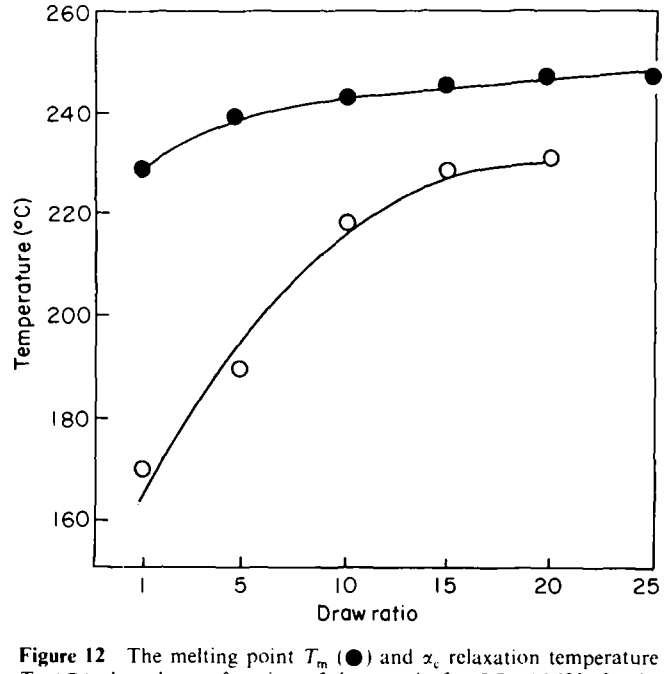

Figure 12 The melting point T_m (●) and α_c relaxation temperature T_{α_c} (○) plotted as a function of draw ratio for $DP = 14400$, 2 wt% PVA/NMP samples

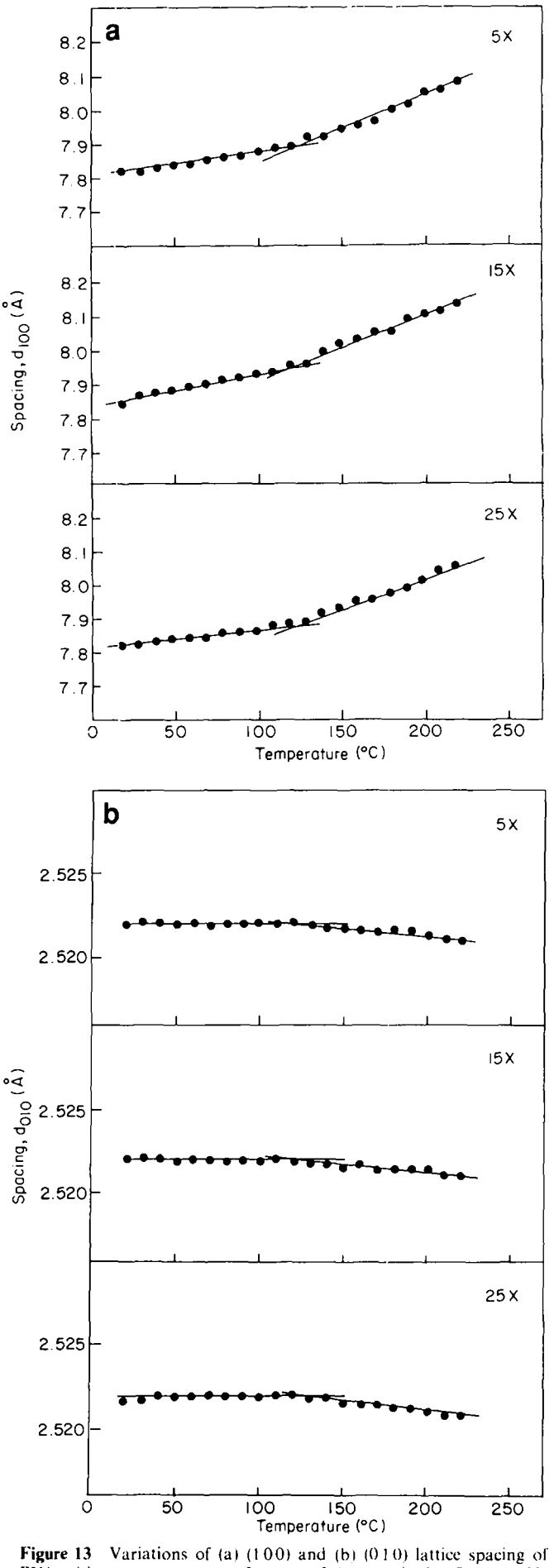

Figure 13 Variations of (a) (1 0 0) and (b) (0 1 0) lattice spacing of PVA with temperature as a function of draw ratio for $DP = 14400$, 2 wt% PVA/NMP samples

drawn samples. However, these figures show that the deflection point due to the second-order transition remains at about 120°C irrespective of draw ratio, and without any indication of other changes in the crystalline chain mobility above 120°C. These results show that the second-order crystal transition is not related to the α_c relaxation, which shifted to higher temperature with draw ratio as shown in *Figure 11*.

Generally, there are two modes of relaxation concerning the crystalline phase: one is due to molecular motion within crystals, while the other is due to that in crystal–amorphous boundaries. Although, Nagai and Takayanagi[25] found that atactic PVA films had two relaxation modes associated with crystalline regions, named β_c and α_c, which are at 130 and 180°C respectively, we observed only an α_c relaxation peak at high temperature. This may be due to the fact that β_c is overlapped by the broad α_c peak in an undrawn sample, and also that β_c relaxation must be difficult to appear in the extensional deformation in the orientation direction of highly drawn samples. This is because the enhancement of frictional movement between chains corresponding to the β_c mode is much reflected in the extension perpendicular to the chain orientation, but not in the parallel direction. This led us to consider that the α_c relaxation is attributed to molecular motion in crystal–amorphous boundaries but not within crystals. While crystal–amorphous boundaries decrease with both increased crystal thickness and crystallinity, high drawing must also result in the tightening of chain packing in the crystal–amorphous boundaries, resulting in the shift of α_c relaxation to higher temperature.

SUMMARY

The gels from PVA/NMP solutions are less crystalline than those from PVA/EG solutions. Dried PVA/NMP gel films have a higher drawability, and the drawn samples have higher modulus at a given draw ratio than those of PVA/EG gel films. These results indicated that the use of solvents with higher solubility towards PVA is advantageous to make gels as a precursor for high drawing.

Although the maximum draw ratio increased with MW of PVA, it was difficult to compare the dependence of drawability on MW with that of UHMWPE, because the highest MW available in this study was about 63×10^4. The largest draw ratio achieved in this study was 28× for dried PVA/NMP films ($DP = 14400$ and 2 wt% gel), and the tensile strength and modulus were 1 GPa and 30 GPa, respectively.

The T_{α_c} estimated from mechanical tan δ shifted to higher temperature, approaching the melting point at high draw ratios, as already observed by Garrett *et al.* for zone-drawn PVA films. Although the shift of T_{α_c} caused during drawing must be related to the difficulty of high drawing of PVA, the thermal expansion of the crystal lattice suggests that the α_c relaxation is not attributed directly to enhanced chain movements within a crystal but to those in crystal amorphous boundaries.

ACKNOWLEDGEMENT

The authors wish to thank Kuraray Co. Ltd, Japan, for supplying the high-molecular-weight PVA samples.

REFERENCES

1 Smith, P. and Lemstra, P. J. *J. Mater. Sci.* 1980, **15**, 505; *Colloid Polym. Sci.* 1980, **258**, 891
2 Cebe, P. and Grubb, D. *J. Mater. Sci.* 1985, **20**, 4465
3 Kavesh, S., Prevorsek, D. C. and Kwon, Y. D. US Patent 1984, 4440711
4 Garrett, P. D. and Grubb, D. T. *Polym. Commun.* 1988, **29**, 60
5 Fujiwara, H., Shibayama, M., Chen, J. H. and Nomura, S. *J. Appl. Polym. Sci.* 1989, **37**, 1403
6 Kunugi, T. and Kawasumi, T. IUPAC Symposium on Macromolecules, Japan, 1988
7 Kiyooka, Y., Tajima, Y. and Kanamoto, T. *Polym. Prepr. Japan* 1988, **37**, 2378
8 Yamaura, K., Tanigami, T. and Matsuzawa, S. *Polym. Prepr. Japan* 1989, **38**, 4400
9 Cha, W. I., Hyon, S. H. and Ikata, Y. *Polym. Prepr. Japan* 1989, **38**, 4406
10 Sakurada, I., Ito, T. and Nakamae, K. *J. Polym. Sci. (C)* 1966, **15**, 75
11 Komotsu, K., Inoue, T. and Miyasaka, K. *J. Polym. Sci., Polym. Phys. Edn.* 1985, **24**, 303
12 Rogovina, L. Z., Slonimskii, G. L., Gembitskii, L. S., Serova, Y. A., Grigor'eva, V. A. and Guberkova, Y. N. *Vysokomol. Soyed. (A)* 1973, **15**, 1411 (*Polym. Sci. USSR* 1973, **15**, 1411)
13 Yamaura, K., Katoh, H., Tanigami, T. and Matsuzawa, S. *J. Appl. Polym. Sci.* 1987, **34**, 2437
14 Bunn, C. W. *Nature* 1948, **161**, 929
15 Scherrer, P. *Gottingen Nachr.* 1918, 98
16 Bragg, W. L., James, R. and Bosanquet, W. *Phil. Mag.* 1921, **41**, 309; 1921, **42**, 1
17 Tubbs, R. K. *J. Polym. Sci. (A)* 1965, **3**, 4181
18 Pritchard, J. G. 'Poly(Vinyl Alcohol): Basic Properties and Use', Gordon and Breach, London, 1970
19 Patel, P., Rodriguez, F. and Moloney, G. *J. Appl. Polym. Sci.* 1979, **23**, 2335
20 Anderyeva, V. M., Anikeyeva, A. A., Lirova, B. I. and Tager, A. A. *Vysokomol. Soyed. (A)* 1973, **15**, 1770 (*Polym. Sci. USSR* 1973, **15**, 1991)
21 Stoks, W. and Berghmans, H. *Br. Polym. J.* 1988, **20**, 316
22 Smith, P. and Lemstra, P. J. *J. Polym. Sci., Polym. Phys. Edn.* 1981, **19**, 1007
23 Garrett, P. D. and Grubb, D. T. *J. Polym. Sci., Polym. Phys. Edn.* 1988, **26**, 2509
24 Shirakashi, K., Ishikawa, K. and Miyasaka, K. *Kobunshikagaku* 1964, **21**, 588
25 Nagai, A. and Takayanagi, M. *Kogyokagakuzashi* 1965, **68**, 96